J. Am. Soc. Mass Spectrom. (2019) 30:2297–2305
DOI: 10.1007/s13361-019-02302-7

RESEARCH ARTICLE

Chiral Differentiation of Non-Covalent Diastereomers Based on Multichannel Dissociation Induced by 213-nm Ultraviolet Photodissociation

Yingying Shi,[1] Min Zhou,[1,2] Kailin Zhang,[1,3] Lifu Ma,[3] Xianglei Kong[1,4]

[1]State Key Laboratory and Institute of Elemento-Organic Chemistry, Nankai University, Tianjin, 300071, China
[2]Department of Physics, Anhui Normal University, Wuhu, 241000, People's Republic of China
[3]School of Precision Instrument and Opto-Electronics Engineering, Tianjin University, Tianjin, 300072, China
[4]Collaborative Innovation Center of Chemical Science and Engineering, Nankai University, Tianjin, 300071, China

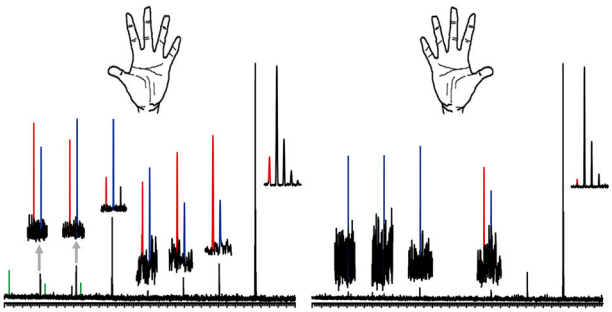

Abstract. Here we present the implementation of 213-nm ultraviolet photodissociation (UVPD) in a FT-ICR mass spectrometer for chiral differentiation in the gas phase. The L/D amino acid–substituted serine octamer ions were selected as examples of diastereoisomers for chiral analysis. Several kinds of fragment ions were observed in these experiments, including fragment ions that are similar to the ones observed in corresponding collision-activated dissociation (CAD) experiments, fragment ions generated with different protonation sites by only destroying non-covalent bonds, and unique non-covalent cluster radical ions. The latter two kinds of fragment ions are found to be more sensitive to the chirality of the substituted units. Further experiments suggest that the formation of radical ions is mainly affected by chromophores on side chains of the substituted units and micro surroundings of the characterized non-covalent diastereoisomers. A comparing experiment performed by only changing the wavelength of UV laser to 266 nm shows that the 213-nm UV laser has the priority in the diversity of fragmentation pathways and potential of further application in chiral differentiation experiments.

Keywords: Chiral differentiation, Ultraviolet photodissociation, Serine octamer, Amino acids, Fragmentation pathways, Radical ions

Received: 14 May 2019/Revised: 10 July 2019/Accepted: 23 July 2019 /Published Online: 13 August 2019

Introduction

Chirality plays a central role throughout the chemical and biological sciences. Enantiomers of organic compounds can exhibit very different pharmacological activities [1]. For example, L-dopa is effective in treating Parkinson's disease, while D-dopa causes serious side effects. Thus, chiral analysis is very important for both fundamental and applied research in chemical and pharmaceutical studies. By now, different approaches, including circular dichroism (CD), nuclear magnetic resonance (NMR), and liquid chromatography (LC) have been widely applied into the field [2–6]. Due to its great performance in speed, sensitivity, and specificity, mass spectrometry (MS) has attracted much interest in the past 20 years in chiral analysis [3–18]. There are two basic points in MS-based chiral analysis experiments. One is how to create a chiral environment; the other is how to distinguish them according to the environment. The first point needs the selection of chiral reference molecules to form diastereomers; the second one needs an effective way to analyze behavioral differences between the non-covalent diastereomers. These differences can be reflected by, for example, the relative abundances of some product ions after ion-molecular reactions or dissociation. By comparing and further analyzing

Electronic supplementary material The online version of this article (https://doi.org/10.1007/s13361-019-02302-7) contains supplementary material, which is available to authorized users.

Correspondence to: Xianglei Kong; *e-mail:* kongxianglei@nankai.edu.cn

their relative mass spectra, both qualitative and quantitative chiral analyses can be performed.

Recently, chiral analysis based on photodissociation mass spectrometry and spectroscopy in the gas phase has attracted much interest [19–26]. Filipp et al. reported the first case of diastereomeric complexes that show clearly different infrared photodissociation (IRPD) spectra [19]. In their research, complex ions of pure enantiomers of bis(diamido)-bridged basket resorcin[4]arene and chiral guest molecules were generated by electrospray ionization (ESI) and studied with the method of the IRPD spectroscopy in the range of 2800–3600 cm^{-1}. As remarkable examples of magic-number molecular clusters, which are also characterized by their strong preference for homochirality, serine octamer and its relatives have been also studied with the method [21–23]. Although understanding the structure of serine octamers is tortuous and difficult, critical progresses have been made with the help of the IRPD method recently [27, 28]. Sel et al. studied the structure of $Ser_8Cl_2^{2-}$ cluster by means of ion mobility spectrometry-mass spectrometry (IMS-MS) and infrared (IR) spectroscopy, and proposed their interesting structure supported by both experimental results and ab initio calculations [27]. Rizzo and coworkers used a combination of cryogenic IR messenger-tagging spectroscopy, room-temperature mid-IR multiple-photon dissociation spectroscopy, and first-principle theory to determine the most stable structure of Ser_8H^+ [28]. IRPD spectroscopy is also applied to the chiral analysis of the serine octamer and its relatives. For instance, Xu and co-workers investigated the chirality recognition of the protonated serine dimer and octamer by the IRPD spectroscopy [21]. Our group also used the ESI-IRPD technology to study the chiral effects of proline and threonine-substituted serine octamers, and achieved the chiral differentiation of substituted units [22, 23]. In addition, chiral differentiation of amino acids using permethylated β-cyclodextrin was also performed with the method in the region of 2650 to 3800 cm^{-1} [24, 25]. Recently, Dopfer et al. applied the method to protonated glutamic acid dimers and probed their chirality recognition in the region of 1100–1900 cm^{-1} and 2600–3600 cm^{-1} [26].

Although the IRPD method can provide some valuable results, it is restricted in some extent by its fragmentation pathway, which is similar to that of CAD experiments. Recently, ultraviolet photodissociation (UVPD) method has been also applied in this field [29–37]. For instance, Fujihara et al. successfully used L-Trp as a chiral probe to achieve the chiral recognition and quantification of monosaccharides with a tandem mass spectrometer equipped with a cold ion trap and a 266-nm Nd:YAG laser [37]. The same group also fulfilled quantitative analysis of leucine and isoleucine [38]. Julian et al. demonstrated the significant utility of the UVPD-initiated radical chemistry in identifying a full suite of glycan isomers [39]. Herein, we apply a tunable UV laser to perform the UVPD mass spectrometry to achieve the chiral differentiation of L/D-amino acids with the homo- and hetero-chiral amino acid–substituted serine octamer ions generated by the ESI. Some interesting and inspiring results were observed by comparing their UVPD mass spectra obtained at 213 nm and 266 nm, respectively. Although the difference in experimental methods between this work and Fujihara's work (213 nm for this present work and 266 nm for Fujihara's work) be thought as small, the difference is noticeable, since the change of the applied UV wavelength makes the dissociation channels more diverse and ready for chiral analysis.

Experimental

Experiments were performed on a 7.0-T Fourier-transform ion cyclotron resonance mass spectrometer (FT-ICR MS) instrument (IonSpec, Varian Inc., Lake Forest, CA, USA). A Z-spray electrospray ionization (ESI) source was used to generate positive ions by applying 3.4 kV to the capillary of the ESI source with respect to the mass spectrometer inlet capillary. A solution of L-serine (3 mM) is prepared in 49:49:2 (v/v) water/methanol/acetic acid solvent. Other solutions, including L/D-Tyr (1 mM), L/D-Trp (1 mM), L/D-Phe (1 mM), L/D-His (1 mM), and L/D-dopa (0.5 mM) are also prepared with the same solvent. Mixed solutions of L-serine with the other amino acids or dopa were then obtained by mixing them with the volume ratio of 1:1 directly. The samples were sprayed at an infusion rate of 1 μL/min. The generated protonated substituted serine octamer ions were injected into an open-ended cylindrical Penning trap via a quadrupole ion guide and mass-selected in the FT ICR cell by the method of stored waveform inverse Fourier transform. Ultraviolet photodissociation (UVPD) mass spectra were obtained using an experimental setup installed recently in our lab. Briefly, a commercial optical parametric oscillator (OPO) laser (EKSPLA, NT-342C, Lithuania) was applied to irradiate the isolated ions in the cell. In experiments reported here, the average laser pulse energy was set at ~ 7 mJ at a frequency of 10 Hz. The pulse duration is 5 ns. The irradiation time was set as 4 s or 8 s which was controlled by a mechanical shutter (Sigma-Koki, Japan). The corresponding CAD mass spectra were obtained using sustained off-resonance irradiation (SORI) excitation with a frequency offset of 1000 Hz [40]. For the experiments of $[\text{L-Ser}_7 + \text{L-Tyr}_1]H^+/[\text{L-Ser}_7 + \text{D-Tyr}_1]H^+$, the $V_{p\text{-}p}$ was set at 3.5 V, while for others, the $V_{p\text{-}p}$ was set at 3.0 V. During each 100-ms SORI event, the interested ions collided with a brief pulse of nitrogen gas.

Results and Discussion

The ESI mass spectra of mixed solutions of L-Ser and L/D-Tyr shown in Figure S1 are similar to the previously reported results [22, 23, 41]. Ions of Ser_8H^+, $[Ser_7 + Tyr_1]H^+$ and $[Ser_6 + Tyr_2]H^+$ can be clearly identified for both L-Tyr and D-Tyr samples. The ions of $[Ser_7 + Tyr_1]H^+$ and $[Ser_6 + Tyr_2]H^+$ were then selected and subjected to CAD and UVPD experiments. The corresponding CAD mass spectra of $[\text{L-Ser}_7 + \text{L-Tyr}_1]H^+$ and $[\text{L-Ser}_7 + \text{D-Tyr}_1]H^+$ are shown in Figure 1a, b, respectively. It can be found that their fragment ions are very similar. Both fragmentation pathways are characterized by the

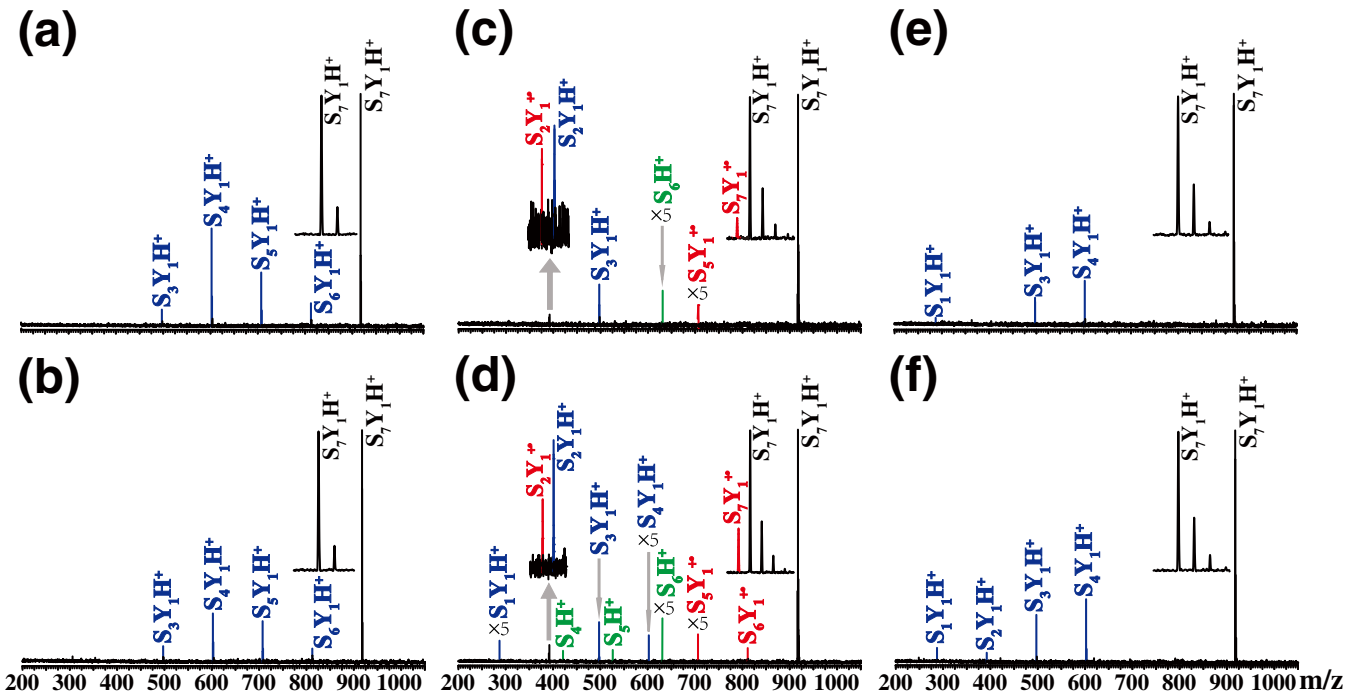

Figure 1. CAD and UVPD@213-nm, and UVPD@266-nm mass spectra of [L-Ser_7 + L-Tyr_1]H^+ (**a**, **c**, **e**) and [L-Ser_7 + D-Tyr_1]H^+ (**b**, **d**, **f**), respectively. The cluster ions of [Ser_n + Tyr_m]H^+ are abbreviated to $S_nY_mH^+$. Some weak peaks have been amplified by 5 times, as shown in the figure

subsequent loss of a unit of L-serine. Differently, the UVPD experiments at 213 nm show some interesting results (Figure 1c, d). First, both radical cations of [L-Ser_7 + L-Tyr_1]$^{+\bullet}$ and [L-Ser_7 + D-Tyr_1]$^{+\bullet}$ were observed in the UVPD mass spectra. The results are somewhat unexpected, since it is usually thought that the non-covalent cluster radical ions are typically unstable and can hardly survive. A careful comparison between the two figures shows that the intensity of [L-Ser_7 + L-Tyr_1]$^{+\bullet}$ is lower than that of [L-Ser_7 + D-Tyr_1]$^{+\bullet}$. Second, the UVPD fragment ions in two cases are quite different. Besides the radical cations of [L-Ser_7 + L-Tyr_1]$^{+\bullet}$ from the precursor ions directly, fragment ions of [L-Ser_{2-3} + L-Tyr_1]H^+, [L-Ser_5 + L-Tyr_1]$^{+\bullet}$, and [L-Ser_2 + L-Tyr_1]$^{+\bullet}$ were also observed. While for the heterochiral cluster of [L-Ser_7 + D-Tyr_1]H^+, the kinds of fragment species are more abundant. Both protonated ions of [L-Ser_{1-4} + D-Tyr_1]H^+ and radical ions of [L-Ser_{5-6} + D-Tyr_1]$^{+\bullet}$ were observed. Third, due to the higher proton affinity (PA) value of Tyr relative to that of Ser [42], no protonated fragment ions consisting only serine unit were observed in their CAD mass spectra. However, in the UVPD mass spectrum of [L-Ser_7 + D-Tyr_1]H^+, the "abnormal" protonated species of [L-Ser_{4-6}]H^+ were also identified, indicating a quite different dissociation pathway. Although this "abnormal" fragment ions generated are probably normal, since the PA value can be changed depending on the chemical environment of the exchange sites in the non-covalent complexes, it is still interesting to find these fragment ions are very useful for the chiral differentiation in the UVPD experiments. And only [L-Ser_6]H^+ can be detected in the case of [L-Ser_7 + L-Tyr_1]H^+. For the UVPD experiments performed at 266 nm, the results are quite different (Figure 1e, f). Similar to the CAD results, only fragment ions of [Ser_{1-4} + Tyr_1]H^+ were observed, and the difference between homochiral and heterochiral clusters is very subtle, which makes chiral differentiation difficult to achieve. Unexpectedly, no radical cluster ions were observed in both cases.

Similar results were observed in the tandem mass spectra of [Ser_6 + Tyr_2]H^+. For CAD mass spectra, only fragment ions of [Ser_{3-5} + Tyr_2]H^+ formed by the subsequent loss of serine unit were observed for both homochiral and heterochiral clusters, as shown in Figure 2a, b. For the UVPD mass spectra obtained at 213 nm, radical ions of [Ser_6 + Tyr_2]$^{+\bullet}$ were observed in both cases. Besides the fragment ions of [Ser_{1-2} + Tyr_2]H^+ and [L-Tyr_2]H^+, non-covalent cluster radical ions of [Ser_5 + Tyr_2]$^{+\bullet}$ were observed in the case of homochiral precursor ions. While for heterochiral precursor ions, only fragment ions of [D-Tyr_2]H^+ were observed. The chiral differentiation can be realized readily by comparing the two mass spectra. However, for the UVPD spectra obtained at 266 nm, no radical ion was observed. The generated fragments were quite similar to each other in both cases (Figure 2e, f).

Considering the choice of UV chromophores, tryptophan was also selected as the substituent unit for further experiments. The results of [Ser_7 + Trp_1]H^+ are shown in Figure 3. As shown in Figure 3a, b, fragment ions of [Ser_{3-6} + Trp_1]H^+ were observed in the CAD mass spectra of [Ser_7 + L/D-Trp_1]H^+ in similar patterns. In their 213-nm UVPD experiments, their spectra are much more different. Although the signal of radical ions of [L-Ser_7 + L-Trp_1]$^{+\bullet}$ is somewhat weak, it is highly recognizable since it is totally absent in the case of heterochiral

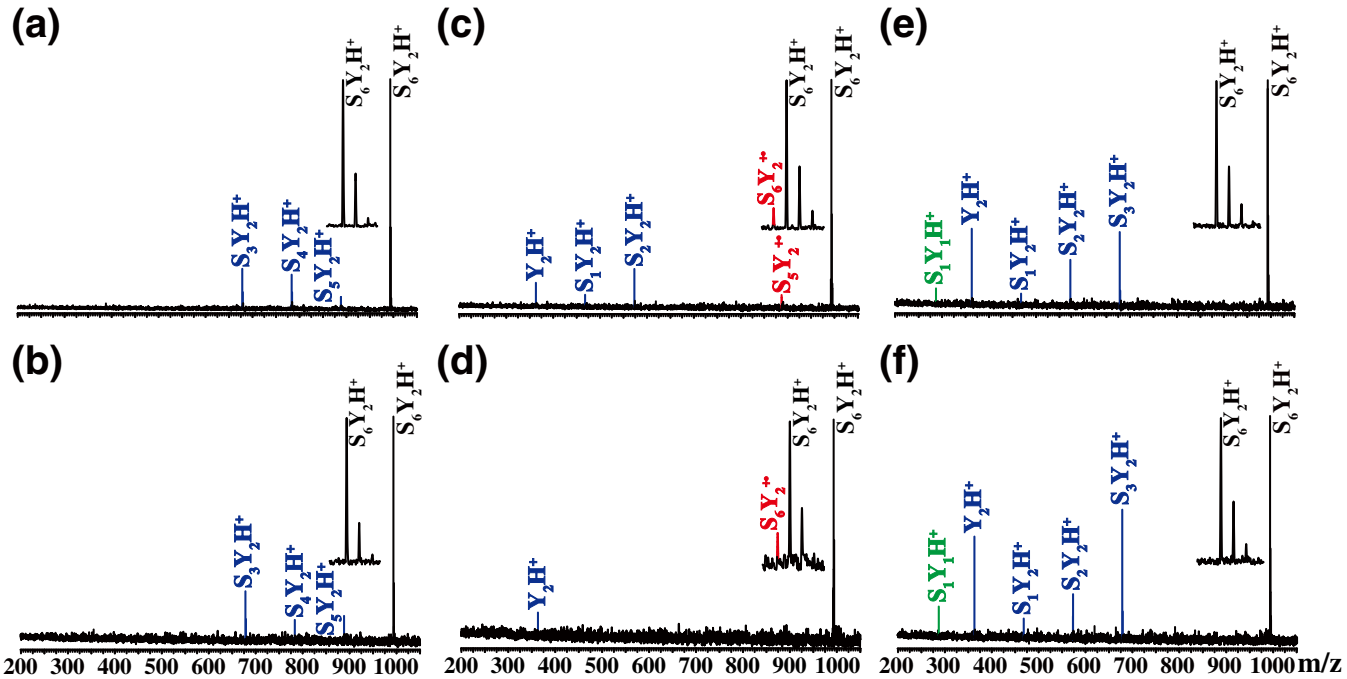

Figure 2. CAD and UVPD@213-nm, and UVPD@266-nm mass spectra of [L-Ser_6 + L-Tyr_2]H^+ (**a**, **c**, **e**) and [L-Ser_6 + D-Tyr_2]H^+ (**b**, **d**, **f**), respectively. The cluster ions of [Ser_n + Tyr_m]H^+ are abbreviated to $S_nY_mH^+$

clusters (Figure 3c, d). In addition, the kinds of fragment ions of [L-Ser_7 + L-Trp_1]H^+ are more abundant than those of [L-Ser_7 + D-Trp_1]H^+. The first series of fragment ions can be defined as the protonated clusters of [L-$Ser_{0–5}$ + L-Trp_1]H^+, which is derived from the subsequent loss of serine unit. The second series is the protonated clusters of [$Ser_{4–6}$]H^+, which are more likely generated with a process of proton transfer. For the heterochiral cluster ions of [L-Ser_7 + D-Trp_1]H^+, only the ions of [L-$Ser_{1–3}$ + D-Trp_1]H^+ from the first series and [Ser_6]H^+ from the second series can be observed. For the 266-nm UVPD

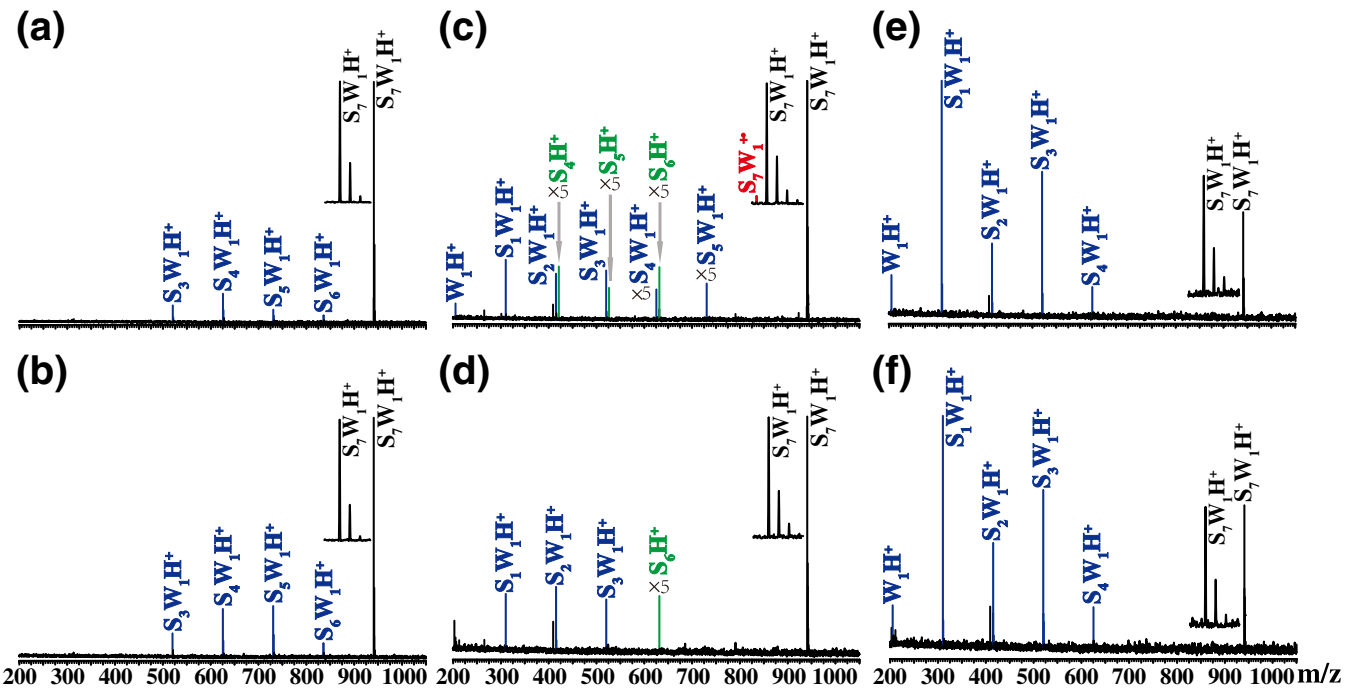

Figure 3. CAD and UVPD@213-nm and UVPD@266-nm mass spectra of [L-Ser_7 + L-Trp_1]H^+ (**a**, **c**, **e**) and [L-Ser_7 + D-Trp_1]H^+ (**b**, **d**, **f**), respectively. The cluster ions of [Ser_n + Trp_m]H^+ are abbreviated to $S_nW_mH^+$. Some weak peaks have been amplified by 5 times, as shown in the figure

experiments, fragment ions of $[Ser_{0–4} + Trp_1]H^+$ were both observed in their mass spectra with similar relative intensities. No radical ions were observed, as shown in Figure 3e, f.

To further verify the effectiveness of 213-nm UVPD mass spectrometry on substituted serine octamers in chiral differentiation, L-dopa and D-dopa were also selected and studied. As an unnatural amino acid, dopa can replace 1 unit of serine in serine octamers readily and the protonated species can be observed in their ESI mass spectra. The double substituted octamer ions, however, are too weak to be isolated for the UVPD in our experiments for both enantiomers. Figure 4 compares the CAD and UVPD mass spectra at 213 nm and 266 nm for L/D-dopa-substituted serine octamers. For CAD experiments, their fragmentation pathways are still characterized by the subsequent loss of 1 unit of serine, resulting in the formation of ions of $[Ser_{4–6} + Dop_1]H^+$. And their 213-nm UVPD mass spectra show quite different results. Interestingly, radical cations of $[Ser_7 + Dop_1]^{+\bullet}$ can be identified for both enantiomers. But the signal of $[Ser_7 + L\text{-}Dop_1]^{+\bullet}$ is much stronger than that of $[Ser_7 + D\text{-}Dop_1]^{+\bullet}$. Also, in the UVPD spectrum of homochiral clusters, three series can be clearly identified. The first series is the protonated clusters of $[Ser_{1–6} + L\text{-}Dop_1]H^+$. These ions are similar to (but more diverse than) those observed in the CAD experiments, thus are suggested to be formed by the subsequent loss of serine unit from the precursor ions. The second series is the protonated clusters of $[Ser_{2–4}]H^+$, which are generated by a different dissociation channel accompanied with a proton transfer process. The third series is the radical ions of $[Ser_{1–6} + L\text{-}Dop_1]^{+\bullet}$. These ions are likely to be dissociated from $[Ser_7 + L\text{-}Dop_1]^{+\bullet}$, which comes from the direct dissociation of the precursor ions. For the heterochiral cluster ions of $[Ser_7 + D\text{-}Dop_1]H^+$, the UVPD spectrum is quite different. The first series ions of $[Ser_{1–3, 5, 6} + D\text{-}Dop_1]H^+$ can still be observed, but total intensities are much weaker than those in the homochiral case. The second series totally disappeared, indicating that the corresponding dissociation channel does not exist in this case. For third series, only weak signal of $[Ser_5 + D\text{-}Dop_1]^{+\bullet}$ can be observed.

For the UVPD of $[Ser_7 + Dop_1]H^+$ at 266 nm, the results are not only different from those at 213 nm, but also different from above the example of $[Ser_7 + Tyr_1]H^+$. For both enantiomers, radical ions of $[Ser_7 + Dop_1]^{+\bullet}$ were observed in the mass spectra with similar relative intensities. Signals of $[Ser_{1, 3, 4, 6} + Dop_1]H^+$ were also observed in the mass spectra. Although the distributions of the series are quite different from those generated in the CAD or 213-nm UVPD experiments, they are very similar to each other for both enantiomers and can be hardly distinguished from each other. For the second kind of ions observed in the 213-nm UVPD spectra, protonated serine dimers were observed in both spectra. The difference between the two spectra is mainly contributed to the third kind of ions. Although ions of $[Ser_3 + Dop_1]^{+\bullet}$ were observed in both results, ions of $[Ser_4 + Dop_1]^{+\bullet}$ can be observed in the experiment of homochiral clusters, indicating their complicated dissociation mechanisms.

However, phenylalanine shows a different example. Without surprise, ions of $[Ser_{4–6} + Phe_1]H^+$ can be identified for both L-Phe- and D-Phe-substituted samples in their CAD mass spectra, as shown in Figure 5a, b. However, no signals of radical cations were observed in all the 213-nm and 266-nm

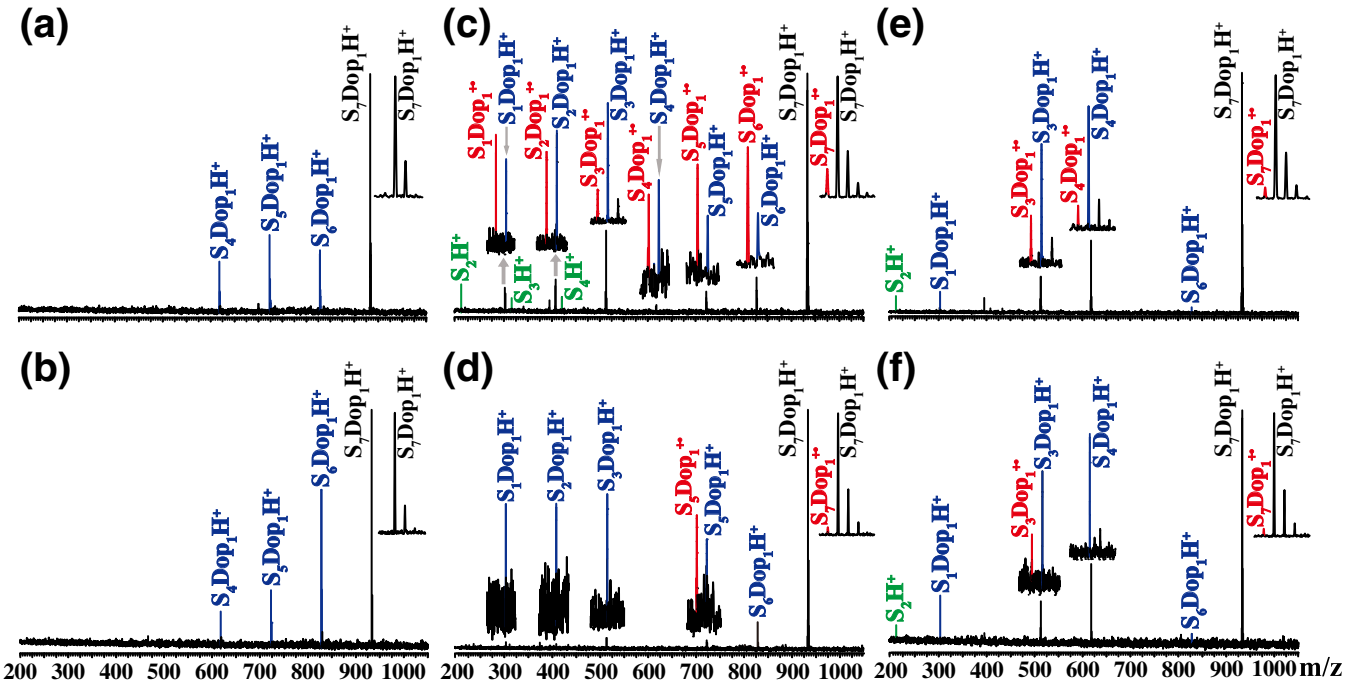

Figure 4. CAD and UVPD@213-nm and UVPD@266-nm mass spectra of $[L\text{-}Ser_7 + L\text{-}Dop_1]H^+$ (**a**, **c**, **e**) and $[L\text{-}Ser_7 + D\text{-}Dop_1]H^+$ (**b**, **d**, **f**). The cluster ions of $[Ser_n + Dop_m]H^+$ are abbreviated to $S_nDop_mH^+$

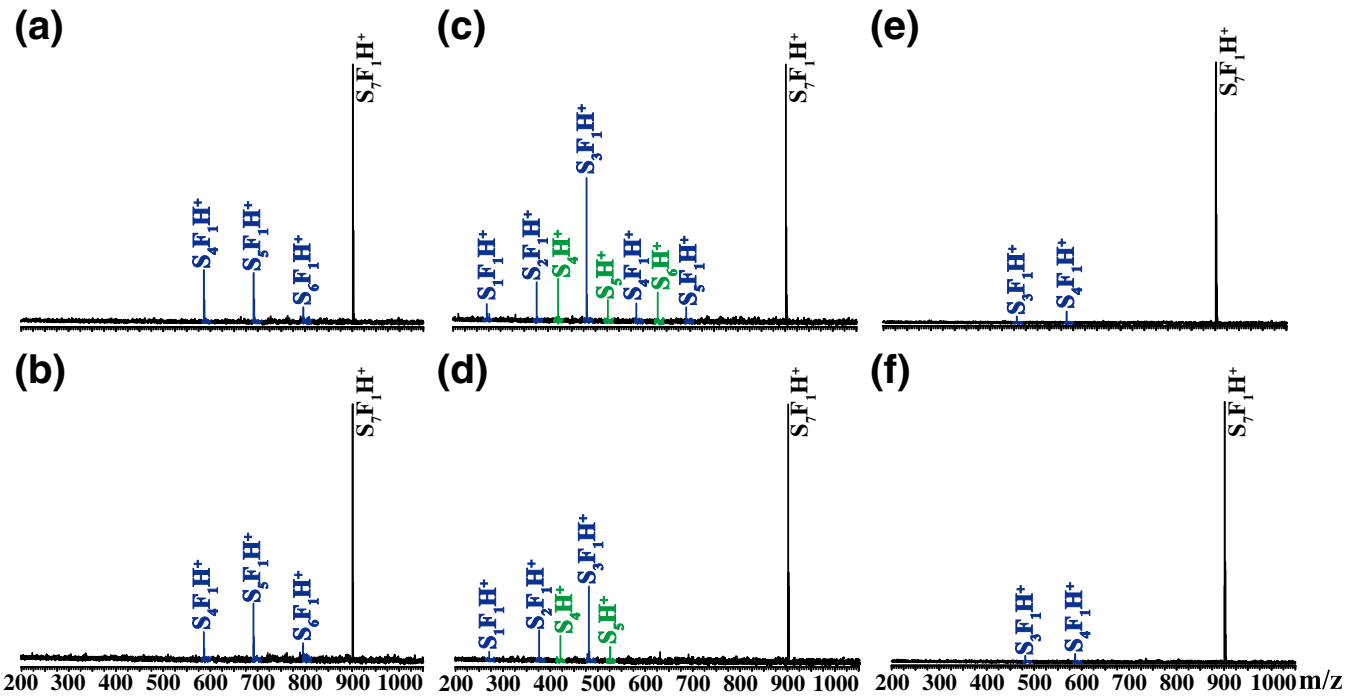

Figure 5. CAD and UVPD@213-nm and UVPD@266-nm mass spectra of [L-Ser_7 + L-Phe_1]H^+ (**a**, **c**, **e**) and [L-Ser_7 + D-Phe_1]H^+ (**b**, **d**, **f**). The cluster ions of [Ser_n + Phe_m]H^+ are abbreviated to $S_nF_mH^+$

UVPD spectra of [L-Ser_7 + L-Phe_1]H^+ and [L-Ser_7 + D-Phe_1]H^+ (Figure 5c–f), although the chiral differentiation still can be fulfilled by their different dissociation patterns at 213 nm.

Surely, it is vital to understand the observed process and how the UV dissociation is linked with chirality. As described above, the generation of radical cations is likely to be very sensitive and important to effective chiral differentiation [43–48]. Since the serine itself has no UV chromophores in this region, its absorption at 213 nm is weak. Fragment ions in the 213-nm UVPD spectra of the Ser_8H^+ are similar to those in CAD spectrum (Figure S2), and no dissociation happened in the 266-nm UVPD experiments. Hence, the origin of the generation of radical cations is derived from the substituent unit rather than serine units. Thus, it is nature to suggest that the 213-nm UVPD behavior of the substituent unit in separated state (instead of in the clusters) should be the key to the generation of the radical cations.

For example, in the case of $TyrH^+$, the H loss due to the direct excitation of the πσ* state was, in fact, observed in the UVPD experiments under wavelengths below 240 nm by Dedonder et al. [49]. And this channel does not exist at 266 nm [50–53]. We also run the UVPD experiment of $TyrH^+$ at 213 and 266 nm separately; the results are consistent, that is, the radical cations by losing one H atom only exists at 213 nm (Figure S3). For $TrpH^+$, several groups have reported its experimental UVPD mass spectra [54–57]. Unlike $TyrH^+$, it has been found the 266-nm UVPD could induce the hydrogen loss for $TrpH^+$ [56–60]. It can be understood as a direct dissociation involving the crossing between a ππ* excited electronic state of the indole and a dissociating πσ* state. Here the UVPD experiment of $TrpH^+$ at 213 and 266 nm was also performed, and the results indicated that in both experiments, the radical cations can be observed clearly (Figure S4). However, it is important to point out that in the UVPD experiment of [L-Ser_7 + L-Trp_1]H^+, the radical cations only appeared in the case of 213 nm, and no such signals were observed at 266 nm (Figure 3c, e). And for [L-Ser_7 + D-Trp_1]H^+, neither of the wavelengths can produce the radical cations (Figure 3d, f). The result strongly indicates the micro surroundings can play an important role in the direct H loss dissociation pathway. The intermolecular hydrogen bonds and salt bridge interaction in the non-covalent complexes have an obvious effect on the structure, electrical energy levels, or dissociation dynamics of the compounds. Correspondingly, the chirality of the substituted unit can also be reflected due to the sensitivity of the dissociation dynamics on the non-covalent interactions. Thus, chiral recognition can be fulfilled based on the enantiomer-selective dissociation pathways under suitable wavelengths.

As far as dopa is concerned, some more interesting results are shown here. For the separated species of protonated L-dopa, radical cations by H loss only appeared in the UVPD mass spectra at 213 nm (Figure S5). However, the ions of [Ser_7 + Dop_1]$^{+\bullet}$ were observed in both wavelengths for both L- and D-dopa, which further demonstrated the effect of the micro surroundings on the substitute unit.

Different from the above examples, in order to form the corresponding H-loss radicals, $PheH^+$ requires more than 6-eV photon energy (which means the wavelength of the UV laser should be below 205 nm) [51]. Here the UVPD experiments of $PheH^+$ at 213 and 266 nm were also performed, and no radical ions were observed (Figure S6). Without surprise, for the Phe substituted serine octamer ions, no radical cations were observed in both the 213- and 266-nm UVPD spectra for both enantiomers of phenylalanine, as shown in Figure 5.

These experimental results also indicate that the side chain of substituent unit plays an important role in chiral recognition and possible enantiomer-selective excitation-induced hydrogen loss. Therefore, chiral differentiation method base on the 213-nm UVPD of substituted-serine octamers suggested here is more likely to be applied when (1) the chiral molecule itself belongs to amino acids or amino acid analogues, in order to form the substituted serine octamer clusters; (2) it has a suitable chromophore in this UV region; and (3) chiral differentiation is better for molecules with side chains including heterocyclic rings or benzene rings attached hetero atoms. To verify the suggestion, histidine was selected and tested. The experimental results were consistent with the expected ones. As shown in Figure S7, radical cations of $[Ser_7 + His_1]^{+\bullet}$ only appeared in the 213-nm UVPD of L-His, which can be applied as the indictor of chiral differentiation. Since the structure of the protonated serine octamers has been recently suggested by Scutelnic et al. [28], it might be performable to find some details about the possible microstructural differences existed in these clusters and their radicals. Here the L/D-tyrosine-substituted serine octamers were selected as an example to be studied. And primary results show that the chiral substituted units might form different structures by replacing different serine unit in both protonated clusters and radicals (Figures S8 and S9). On the other hand, although the experiments reported here are only about these serine octamer ions, we still think it is reasonable to believe the method of the 213-nm UVPD can be applied as a versatile one for tandem mass spectrometry of cluster ions aimed at chiral analysis by selecting suitable chiral ligand, which has a right chromophores and sensitive dissociation dynamics to its non-covalent interactions. In the meantime, other clusters with homochiral or heterochiral preferences [61–64] might broaden the application of the method. However, it should also be pointed out that the observed dissociative complexity and some unpredictable UVPD dissociation behaviors may somewhat limit its application.

It is also important to point out that other experimental facts may also affect the results of chiral analysis. For example, temperature might affect the non-covalent structures greatly. As previously reported by Fujihara et al. [29–38], the population distribution of non-covalent structures was depending on temperature above 170 K. Since higher temperatures are likely to increase the complexity of the configuration of complex ions, experiment performed under lower temperatures might be a better choice. But this needs the experimental setup to be equipped with extra part providing low temperatures. And other experimental conditions including ionization source, voltage, and solution can influence the complex ions too [65]. The R_{chiral} values of the method can also be calculated according to $R_{chiral} = R_D/R_L$, in which the values of R_D and R_L can be defined using similar ways as previously suggested [9–11, 66]. These results are listed in the Table S1, showing the great advantages of the method. However, considering the complex fragmentation patterns, there will be still a lot of jobs need to do in order to make the quantitative analysis for real samples based on the method practically performable.

Conclusions

In summary, we report that the method of the 213-nm UVPD mass spectrometry can be applied to chiral differentiation effectively. Singly or doubly substituted serine octamer ions were generated by the ESI and isolated for the 213-nm UVPD experiments. The chirality of the substituted unit(s) can affect the UV-induced cleavage of the non-covalent gas-phase complexes greatly. Chiral differentiation can be performed readily according to their different dissociation patterns. Especially, the different fragment ions generated from the break of non-covalent bonds but with a different protonation site from fragment ions observed in the CAD experiments, and the unique non-covalent cluster radical ions provide valuable information and may be applied as the key for achieving chiral differentiation readily. In general, the micro surroundings including the intermolecular hydrogen bonds inside the clusters and salt bridge interaction of non-covalent complexes and the side chains of the substituted units are major factors influencing the formation of radical ions and the chiral differentiation. Therefore, chiral differentiation method base on the 213-nm UVPD of substituted-serine octamers units suggested here may satisfy amino acids and their analogues with suitable chromophores in side chains, such as heterocyclic rings. Considering the increasing ability for the generation of non-covalent complexes with the ESI and other novel soft ionization methods, and the rapidly developing technologies in different kinds of tandem mass spectrometers, the potential of the present method for fast chiral analysis or other structural isomer analyses related to biological and environmental samples is very attractive and promising.

Acknowledgements

Financial support from the National Natural Science Foundation of China (Nos. 21627801, 21475065) is gratefully acknowledged.

Author Contributions

The manuscript was written through contributions of all authors. All authors have given approval to the final version of the manuscript.

Compliance with Ethical Standards

Conflict of Interest The authors declare that they have no competing interests.

References

1. Nguyen, L.A., He, H., Pham-Huy, C.: Chiral drugs: an overview. Int. J. Biomed. Sci. **2**, 85–100 (2006)
2. Ward, T.J., Baker, B.A.: Chiral separations. Anal. Chem. **80**, 4363–4372 (2008)
3. Tao, W.A., Cooks, R.G.: Chiral analysis by MS. Anal. Chem. **75**, 25A–31A (2003)

4. Wu, L., Vogt, F.G.: A review of recent advances in mass spectrometric methods for gas-phase chiral analysis of pharmaceutical and biological compounds. J. Pharm. Biomed. Anal. **69**, 133–147 (2012)
5. Awad, H., El-Aneed, A.: Enantioselectivity of mass spectrometry: challenges and promises. Mass Spectrom. Rev. **32**, 466–483 (2013)
6. Yu, X., Yao, Z.P.: Chiral recognition and determination of enantiometric excess by mass spectrometry: a review. Anal. Chim. Acta. **968**, 1–20 (2017)
7. Sawada, M., Takai, Y., Kaneda, T., Arakawa, R., Okamoto, M., Doe, H., Matsuo, T., Naemura, K., Hirose, K., Tobe, Y.: Chiral molecular recognition in electrospray ionization mass spectrometry. Chem. Commun. **0**, 1735–1736 (1996)
8. Ramirez, J., He, F., Lebrilla, C.B.: Gas-phase chiral differentiation of amino acid guests in cyclodextrin hosts. J. Am. Chem. Soc. **120**, 7387–7388 (1998)
9. Tao, W.A., Zhang, D., Wang, F., Thomas, P.D., Cooks, R.G.: Kinetic resolution of D, L-amino acids based on gas-phase dissociation of copper(II) complexes. Anal. Chem. **71**, 4427–4429 (1999)
10. Tao, W.A., Zhang, D., Nikolaev, E.N., Cooks, R.G.: Copper(II)-assisted enantiomeric analysis of D, L-amino acids using the kinetic method: chiral recognition and quantification in the gas phase. J. Am. Chem. Soc. **122**, 10598–10609 (2000)
11. Yao, Z.P., Wan, T.S.M., Kwong, K.P., Che, C.T.: Chiral analysis by electrospray ionization mass spectrometry/mass spectrometry. 1. Chiral recognition of 19 common amino acids. Anal. Chem. **72**, 5383–5393 (2000)
12. Yao, Z.P., Wan, T.S.M., Kwong, K.P., Che, C.T.: Chiral analysis by electrospray ionization mass spectrometry/mass spectrometry. 2. Determination of enantiomeric excess of amino acids. Anal. Chem. **72**, 5394–5401 (2000)
13. Liu, Q., Zhang, S.Z., Wu, B.D., Guo, J.F., Xie, J.W., Gu, M.S., Zhao, Y.M., Yun, L.H., Liu, K.L.: Chiral melamine derivatives: design, synthesis, and application to mass spectrometry based chiral analysis. Anal. Chem. **77**, 5302–5310 (2005)
14. Enders, J.R., McLean, J.A.: Chiral and structural analysis of biomolecules using mass spectrometry and ion mobility-mass spectrometry. Chirality. **21**, E253–E264 (2009)
15. Kong, X.L.: Chiral differentiation of amino acids by the kinetic method by Fourier transform ion cyclotron resonance mass spectrometry via a different dissociation pathway. Rapid Commun. Mass Spectrom. **26**, 870–873 (2012)
16. Piovesana, S., Samperi, R., Lagana, A., Bella, M.: Determination of enantioselectivity and enantiomeric excess by mass spectrometry in the absence of chiral chromatographic separation: an overview. Chem. Eur. J. **19**, 11478–11494 (2013)
17. Kong, X.L., Huo, Z.Y., Zhai, W.: Chiral differentiation of amino acids by in source collision-induced dissociation mass spectrometry. Mass Spectrom. **3**, S0031 (2014)
18. Bain, R.M., Yan, X., Raab, S.A., Ayrton, S.T., Flick, T.G., Cooks, R.G.: On-line chiral analysis using the kinetic method. Analyst. **141**, 2441–2446 (2016)
19. Filippi, A., Fraschetti, C., Piccirillo, S., Rondino, F., Botta, B., D'Acquarica, I., Calcaterra, A., Speranza, M.: Chirality effects on the IRMPD spectra of basket resorcinarene/ nucleoside complexes. Chem. Eur. J. **18**, 8320–8328 (2012)
20. Rondino, F., Ciavardini, A., Satta, M., Paladini, A., Fraschetti, C., Filippi, A., Botta, B., Calcaterra, A., Speranza, M., Giardini, A., Piccirillo, S.: Ultraviolet and infrared spectroscopy of neutral and ionic non-covalent diastereomeric complexes in the gas phase. Rend. Fis. Acc. Lincei. **24**, 259–267 (2013)
21. Sunahori, F.X., Yang, G.C., Kitova, E.N., Klassen, J.S., Xu, Y.J.: Chirality recognition of the protonated serine dimer and octamer by infrared multiphoton dissociation spectroscopy. Phys. Chem. Chem. Phys. **15**, 1873–1886 (2013)
22. Liao, G.H., Yang, Y.J., Kong, X.L.: Chirality effects on proline-substituted serine octamers revealed by infrared photodissociation spectroscopy. Phys. Chem. Chem. Phys. **16**, 1554–1558 (2014)
23. Ren, J., Wang, Y.Y., Feng, R.X., Kong, X.L.: Investigation of L/D-threonine substituted L-serine octamer ions by mass spectrometry and infrared photodissociation spectroscopy. Chin. Chem. Lett. **28**, 537–540 (2017)
24. Lee, S.S., Park, S., Yin, H., Lee, J., Kim, J.H., Yoon, D., Kong, X., Lee, S., Oh, H.B.: Chiral differentiation of D- and L-alanine by permethylated β-Cyclodextrin: IRMPD spectroscopy and DFT methods. Phys. Chem. Chem. Phys. **19**, 14729–14737 (2017)
25. Lee, S.S., Lee, J., Oh, J.H., Park, S., Yin, H., Min, B.K., Lee, H.H.L., Kim, H.I., Kong, X., Lee, S., Oh, H.B.: Chiral differentiation of D- and L-isoleucine using permethylated β-Cyclodextrin: infrared multiple photon dissociation spectroscopy, ion-mobility mass spectrometry, and DFT calculations. Phys. Chem. Chem. Phys. **20**, 30428–30436 (2018)
26. Klyne, J., Bouchet, A., Ishiuchi, S., Fujii, M., Schneider, M., Baldauf, C., Dopfer, O.: Probing chirality recognition of protonated glutamic acid dimers by gas-phase vibrational spectroscopy and first-principles simulations. Phys. Chem. Chem. Phys. **20**, 28452–28464 (2018)
27. Seo, J., Warnke, S., Pagel, K., Bowers, M.T., von Helden, G.: Infrared spectrum and structure of the homochiral serine octamer-dichloride complex. Nat. Chem. **9**, 1263–1268 (2017)
28. Scutelnic, V., Perez, M.A.S., Marianski, M., Warnke, S., Gregor, A., Rothlisberger, U., Bowers, M.T., Baldauf, C., von Helden, G., Rizzo, T.R., Seo, J.: The structure of the protonated serine octamer. J. Am. Chem. Soc. **140**, 7554–7560 (2018)
29. Fujihara, A., Maeda, N., Hayakawa, S.: Enantiomer-selective photolysis of cold gas-phase tryptophan in L-serine clusters with linearly polarized light. Orig. Life Evol. Biosph. **44**, 67–73 (2014)
30. Fujihara, A., Sato, T., Hayakawa, S.: Enantiomer-selective ultraviolet photolysis of temperature-controlled protonated tryptophan on a chiral crown ether in the gas phase. Chem. Phys. Lett. **610-611**, 228–233 (2014)
31. Fujihara, A., Maeda, N., Hayakawa, S.: Quantitative chiral analysis of tryptophan using enantiomer-selective photolysis of cold non-covalent complexes in the gas phase. J. Mass Spectrom. **50**, 451–453 (2015)
32. Fujihara, A., Maeda, N., Hayakawa, S.: Enantioselective photolysis and quantitative chiral analysis of tryptophan complexed with alkali-metalized L-serine in the gas phase. Chirality. **27**, 349–352 (2015)
33. Fujihara, A., Maeda, N., Hayakawa, S.: Chiral recognition between L-alanine peptides and tryptophan enantiomers probed by ultraviolet photodissociation in the gas phase. J. Mass Spectrom. **51**, 257–260 (2016)
34. Fujihara, A., Maeda, N., Doan, T.N., Hayakawa, S.: Enantiomeric excess determination for monosaccharides using chiral transmission to cold gas-phase tryptophan in ultraviolet photodissociation. J. Am. Soc. Mass Spectrom. **28**, 224–228 (2017)
35. Fujihara, A., Maeda, N.: Quantitative chiral analysis of amino acids in solution using enantiomer-selective photodissociation of cold gas-phase tryptophan via chiral recognition. Anal. Chim. Acta. **979**, 31–35 (2017)
36. Fujihara, A., Inoue, H., Sogi, M., Tajiria, M., Wada, Y.: Chiral and molecular recognition through protonation between aromatic amino acids and tripeptides probed by collision-activated dissociation in the gas phase. Molecules. **23**, 162 (2018)
37. Fujihara, A., Okawa, Y.: Chiral and molecular recognition of monosaccharides by photoexcited tryptophan in cold gas-phase noncovalent complexes as a model for chemical evolution in interstellar molecular clouds. Anal. Chim. Acta. **410**, 6279–6287 (2018)
38. Oki, N., Fujihara, A.: Molecular recognition and quantitative analysis of leucine and isoleucine using photodissociation of cold gas-phase noncovalent complexes. J. Mass Spectrom. **53**, 595–597 (2018)
39. Riggs, D.L., Hofmann, J., Hahm, H.S., Seeberger, P.H., Pagel, K., Julian, R.R.: Glycan isomer identification using ultraviolet photodissociation initiated radical chemistry. Anal. Chem. **90**, 11581–11588 (2018)
40. Gauthier, J.W., Trautman, T.R., Jacobson, D.B.: Sustained off-resonance irradiation for collision-activated dissociation involving Fourier-transform mass spectrometry collision-activated dissociation technique that emulates infrared multiphoton dissociation. Anal. Chim. Acta. **246**, 211–225 (1991)
41. Nanita, S.C., Cooks, R.G.: Serine octamers: cluster formation, reactions, and implications for biomolecule homochirality. Angew. Chem. Int. Ed. **45**, 554–569 (2006)
42. Bleiholder, C., Suhai, S., Paizs, B.: Revising the proton affinity scale of the naturally occurring α-amino acids. J. Am. Soc. Mass Spectrom. **17**, 1275–1281 (2006)
43. Tabarin, T., Antoine, R., Broyer, M., Dugourd, P.: Specific photodissociation of peptides with multi-stage mass spectrometry. Rapid Commun. Mass Spectrom. **19**, 2883–2892 (2005)
44. Sun, Q.Y., Nelson, H., Ly, T., Stoltz, B.M., Julian, R.R.: Side chain chemistry mediates backbone fragmentation in hydrogen deficient peptide radicals. J. Proteome Res. **8**, 958–966 (2009)
45. Halim, M.A., Girod, M., MacAleese, L., Lemoine, J., Antoine, R., Dugourd, P.: 213nm ultraviolet photodissociation on peptide anions:

radical-directed fragmentation patterns. J. Am. Soc. Mass Spectrom. **27**, 474–486 (2016)
46. Nguyen, H.T.H., Shaffer, C.J., Turecek, F.: Probing peptide cation-radicals by near- UV photodissociation in the gas phase. Structure elucidation of histidine radical chromophores formed by near-UV photodissociation in the gas phase. Structure elucidation of histidine radical chromophores formed by electron transfer reduction. J. Phys. Chem. B. **119**, 3948–3961 (2015)
47. Herburger, A., van der Linde, C., Beyer, M.K.: Photodissociation spectroscopy of protonated leucine encephalin. Phys. Chem. Chem. Phys. **19**, 10786–10795 (2017)
48. Cooper, G.A., Hansen, C.S., Karsili, T.N.V., Ashfold, M.N.R.: Photofragment translational spectroscopy studies of H atom loss following ultraviolet photoexcitation of methimazole in the gas phase. J. Phys. Chem. A. **122**, 9869–9878 (2018)
49. Dedonder, C., Feraud, G., Jouvet, C.: In: Nielsen, S.B., Wyer, J.A. (eds.) Photophysics of Ionic Biochromophores, pp. 155–180. SpringerVerlag and Co.: Berlin and Heidelberg GmbH (2013)
50. Soorkia, S., Broquier, M., Gregoire, G.: Conformer- and mode-specific excited state lifetimes of cold protonated tyrosine ions. J. Phys. Chem. Lett. **5**, 4349–4355 (2014)
51. Feraud, G., Broquier, M., Dedonder-Lardeux, C., Jouvet, C., Gregoire, G., Soorkia, S.: Excited state dynamics of protonated phenylalanine and tyrosine: photo-induced reactions following electronic excitation. J. Phys. Chem. A. **119**, 5914–5924 (2015)
52. Gregoire, G., Jouvet, C., Dedonder, C., Sobolewski, A.L.: Ab initio study of the excited-state deactivation pathways of protonated tryptophan and tyrosine. J. Am. Chem. Soc. **129**, 6223–6231 (2007)
53. Kang, H., Jouvet, C., Dedonder-Lardeux, C., Martrenchard, S., Gregoire, G., Desfrancois, C., Schermann, J.P., Barat, M., Fayeton, J.A.: Ultrafast deactivation mechanisms of protonated aromatic amino acids following UV excitation. Phys. Chem. Chem. Phys. **7**, 394–398 (2005)
54. Nolting, D., Marian, C., Weinkauf, R.: Protonation effect on the electronic spectrum of tryptophan in the gas phase. Phys. Chem. Chem. Phys. **6**, 2633–2640 (2004)
55. Talbot, F.O., Tabarin, T., Antoine, R., Broyer, M., Dugourd, P.: Photodissociation spectroscopy of trapped protonated tryptophan. J. Chem. Phys. **122**, 074310 (2005)
56. Kang, H., Dedonder-Lardeux, C., Jouvet, C., Martrenchard, S., Gregoire, G., Desfrancois, C., Schermann, J.P., Barat, M., Fayeton, J.A.: Photo-induced dissociation of protonated tryptophan TrpH(+): a direct dissociation channel in the excited states controls the hydrogen atom loss. Phys. Chem. Chem. Phys. **6**, 2628–2632 (2004)
57. Boyarkin, O.V., Mercier, S.R., Kamariotis, A., Rizzo, T.R.: Electronic spectroscopy of cold protonated tryptophan and tyrosine. J. Am. Chem. Soc. **128**, 2816–2817 (2006)
58. Lepere, V., Lucas, B., Barat, M., Fayeton, J.A., Picard, Y.J., Jouvet, C., Çarcabal, P., Nielsen, I.B., Dedonder-Lardeux, C., Gregoire, G., Fujii, A.: Characterization of neutral fragments issued from the photodissociation of protonated tryptophane. Phys. Chem. Chem. Phys. **9**, 5330–5334 (2007)
59. Lucas, B., Barat, M., Fayeton, J.A., Perot, M., Jouvet, C., Gregoire, G., Brøndsted Nielsen, S.: Mechanisms of photoinduced C-alpha-C-beta bond breakage in protonated aromatic amino acids. J. Chem. Phys. **128**, 164302 (2008)
60. Gregoire, G., Lucas, B., Barat, M., Fayeton, J.A., Dedonder-Lardeux, C., Jouvet, C.: UV photoinduced dynamics in protonated aromatic amino acid. Eur. Phys. J. D. **51**, 109–116 (2009)
61. Myung, S., Fioroni, M., Julian, R.R., Koeniger, S.L., Baik, M., Clemmer, D.E.: Chirally directed formation of nanometer-scale proline clusters. J. Am. Chem. Soc. **128**, 10833–10839 (2006)
62. Atlasevich, N., Holliday, A.E., Valentine, S.J., Clemmer, D.E.: Chirality and packing in small proline clusters. J. Phys. Chem. B. **116**, 11442–11446 (2012)
63. Holliday, A.E., Atlasevich, N., Myung, S., Plasencia, M.D., Valentine, S.J., Clemmer, D.E.: Oscillations of chiral preference in proline clusters. J. Phys. Chem. A. **117**, 1035–1041 (2013)
64. Ma, L., Ren, J., Feng, R., Zhang, K., Kong, X.: Structural characterizations of protonated homodimers of amino acids: revealed by infrared multiple photon dissociation (IRMPD) spectroscopy and theoretical calculations. Chin. Chem. Lett. **29**, 1333–1339 (2018)
65. Kong, X.L., Lin, C., Infusini, G., Oh, H.B., Jiang, H.H., Breuker, K., Wu, C.C., Charkin, O.P., Chang, H.C., McLafferty, F.W.: Numerous isomers of serine octamer ions characterized by infrared photodissociation spectroscopy. ChemPhysChem. **10**, 2603–2606 (2009)
66. Tao, Y.Q., Julian, R.R.: Identification of amino acid epimerization and isomerization in crystallin proteins by tandem LC-MS. Anal. Chem. **86**, 9733–9741 (2014)